Automated validation report for PyWake

DTU Wind Energy
E-report

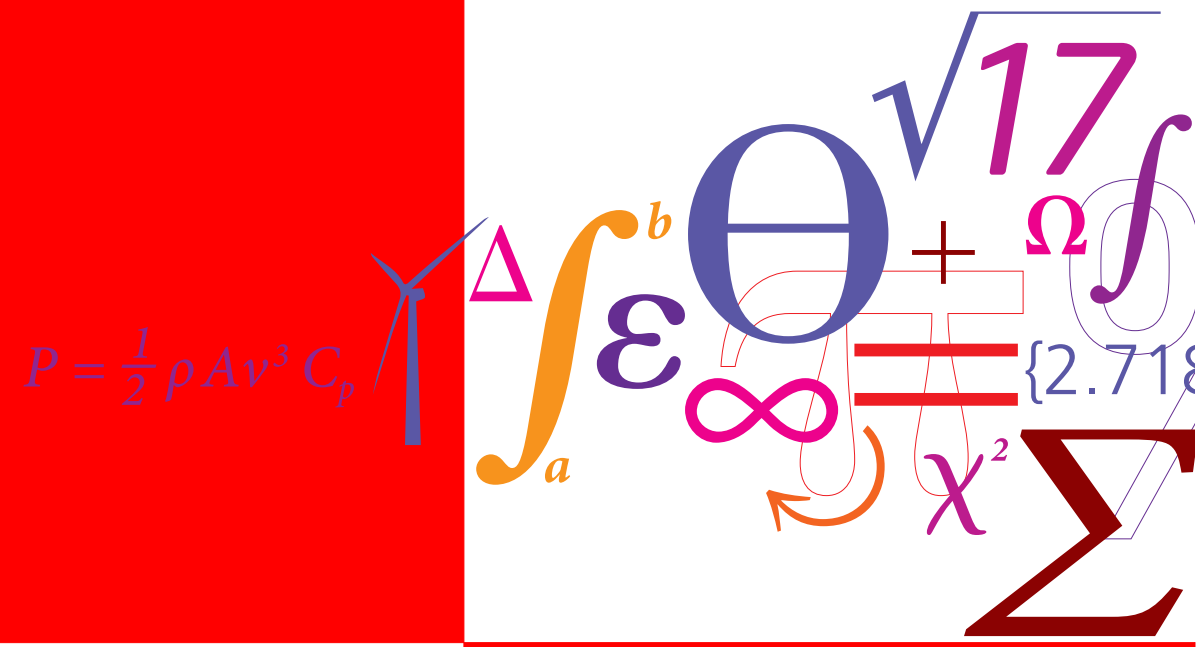

PyWake development team

DTU Wind Energy E-XXXX
March 2023

DTU Wind Energy
Department of Wind Energy

1 Introduction

This report is an automatically generated document used for validation of the wake models available in PyWake.

2 Model description

The following engineering wake models of PyWake are tested:

- GAU - Gaussian wake model of Bastankhah and Porté-Agel (2014) with:
  - Quadratic wake summation.
  - Wake expansion parameter k defined by the stream-wise ambient turbulence intensity at hub height $I_{u,H,\infty}$: $k = 0.4I_{u,H,\infty} + 0.004$ for $0.065 \leq I_{u,H,\infty} \leq 0.15$ following Niayifar and Porté-Agel (2015). Outside this range we set constant k values: for $I_{u,H,\infty} < 0.065$, $k = 0.03$ and for $I_{u,H,\infty} > 0.15$, $k = 0.064$.
- NOJ - Top hat wake model of Jensen (1983) with:
  - Quadratic wake summation.
  - The wake expansion parameter k is 0.04 and 0.1 for the offshore and onshore cases, respectively.

The following higher fidelity wake models are used as references:

- LES - Large-eddy simulations from van der Laan et al. (2015b).
- RANS - Reynolds-averaged Navier-Stokes simulations from van der Laan et al. (2015b) and van der Laan et al. (2015a).

3 Test cases

The test cases used to validate the wake models are listed in Table 1. The first six test case are based on field measurements of the velocity deficit of single wind turbine wakes. Cases 7-13 are based on Supervisory Control And Data Acquisition (SCADA) measurements of the power in wind turbines rows within wind farms. Details of the single wake and wind farm cases and be found in van der Laan et al. (2015b) and van der Laan et al. (2015a), respectively. Note that Table 1 lists the total ambient turbulence intensity $I_{H,\infty}$, which is about 80% of the stream-wise turbulence intensity.

Single wake cases

Case	Description	Measurement data	$I_{H,\infty}$ [%]	C_T [-]	$U_{H,\infty}$ [m/s]	D [m]	z_H [m]
1	Wieringermeer West	Met. mast, 4.5 years, $3.5D$	8.0	0.63	10.7	80	80
2	Wieringermeer East	Met. mast, 4.5 years, $2.5D$	6.0	0.63	10.9	80	80
3	Nibe B	Met. mast, 2 years, $2.5, 4, 7.5D$	8.0	0.89	8.5	40	45
4	Nordtank 500	Lidar, 102x10 minutes, $2, 5D^*$	11.2	0.70	7.45	41	36
5	NREL-5MW Low $I_{H,\infty}$	-	4.0	0.79	8.0	126	90
6	NREL-5MW High $I_{H,\infty}$	-	12.8	0.79	8.0	126	90

Wind farm cases

Case	Description	Measurement data (SCADA)	$I_{H,\infty}$ [%]	s [D]	$U_{H,\infty}$ [m/s]	D [m]	z_H [m]
7	Wieringermeer	wd=275°±2.5°	9.6	3.8	8.35	80	80
8	Lillgrund south-west aligned	wd=222°±2.5°, rows B and D	4.8	4.3	9	92.6	65
9	Lillgrund south-west staggered	wd=207°±2.5°, rows B and D	4.8		9	92.6	65
10	Lillgrund south-east aligned	wd=120°±2.5°, rows 4 and 6	4.8	3.2	9	92.6	65
11	Lillgrund south-east staggered	wd=105°±2.5°, rows 4 and 6	4.8		9	92.6	65
12	Lillgrund efficiency	all wd ±1.5°	4.8		9	92.6	65
13	Horns Rev I	wd=270°±2.5°, rows 2-7	5.6	7.0	8	80.0	70

Table 1: Summary of test cases. $I_{H,\infty}$ is the ambient total turbulence intensity at hub height based on the turbulent kinetic energy, C_T is the thrust coefficient, $U_{H,\infty}$ is the free-stream velocity at hub height, D is the rotor diameter, z_H is the hub height, s is the effective inter wind turbine spacing in a wind farm for a row-aligned wind direction (wd).

3.1 Results

The results of the measurements include errors bars, representing the statistical uncertainty of the mean ($\sigma/\sqrt{n}$, where σ is the standard deviation of the all 10 min. averaged values and $\sqrt{n}$ is the number of 10 min. averaged values). This procedure makes the errors quite small if the number of 10 min. is large. Note that the standard deviations of the Nibe single wake case are not available.

3.1.1 Single wake cases

The LES results in the single wake cases are shown as shaded areas, which represent the statistical uncertainty of the mean of six consecutive 10 min. bins (1 hour LES data).

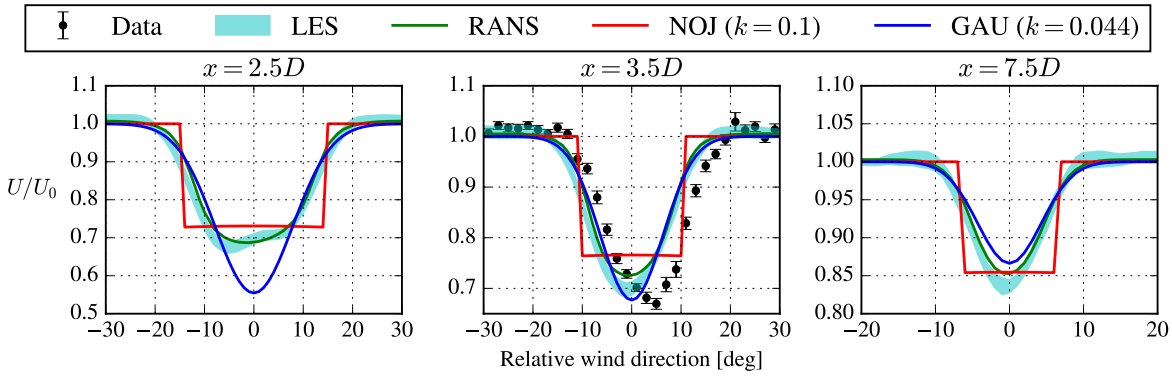

Figure 1: Case 1: Wieringermeer-West.

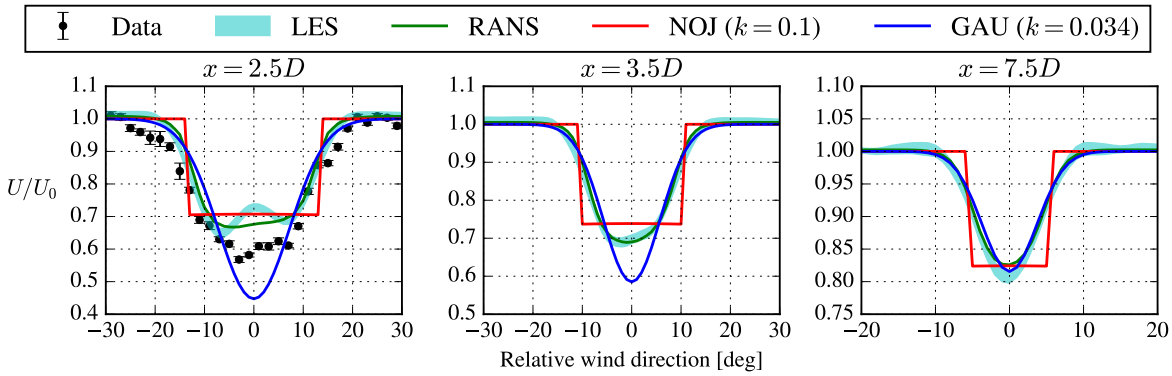

Figure 2: Case 2: Wieringermeer-East.

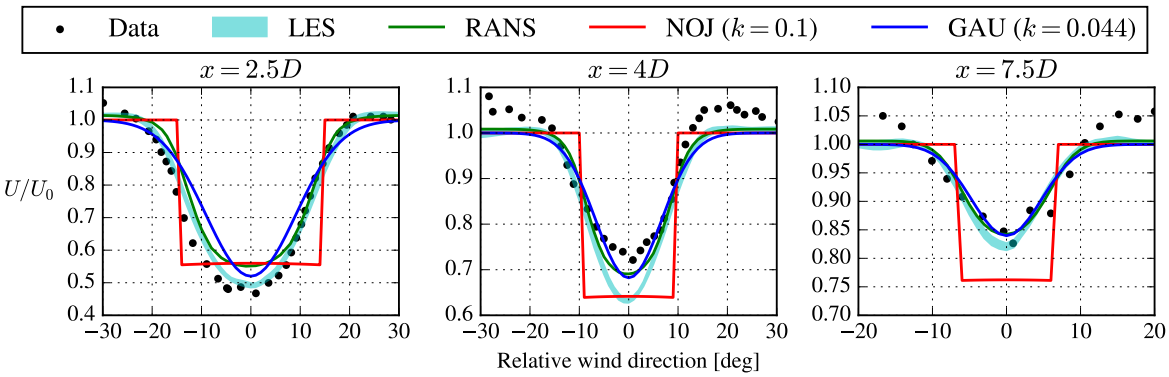

Figure 3: Case 3: Nibe B.

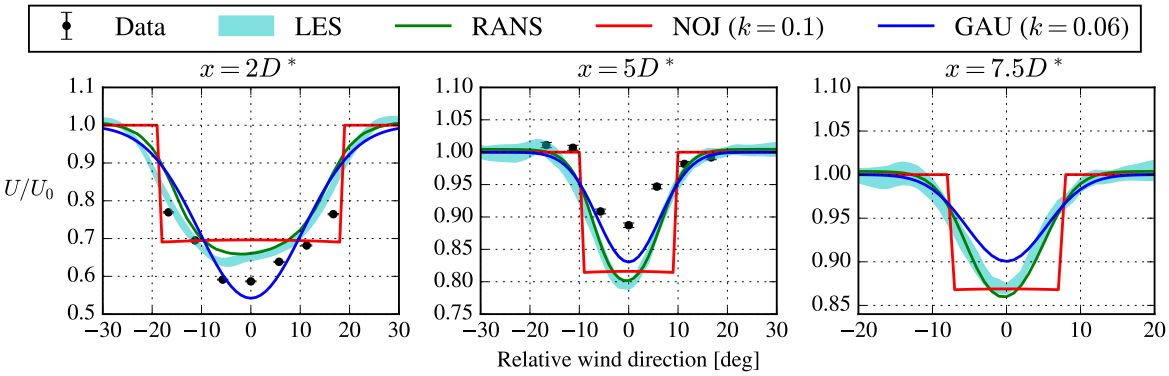

Figure 4: Case 4: Nordtank-500.

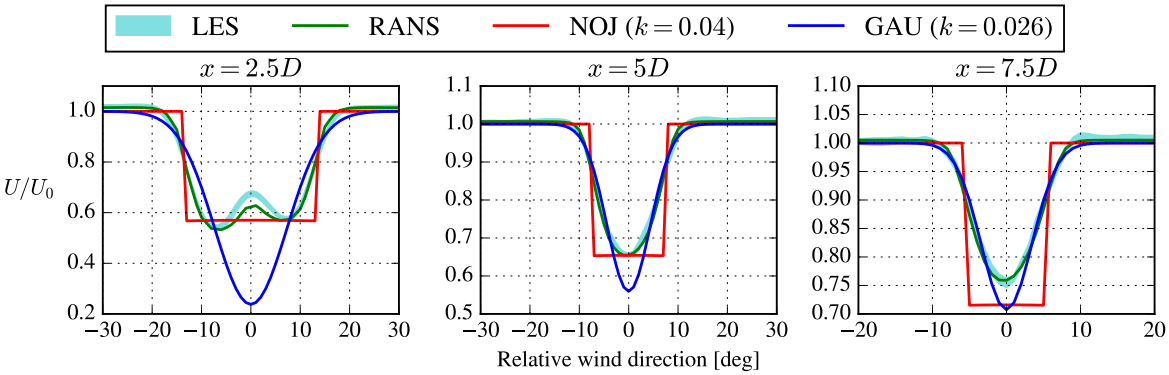

Figure 5: Case 5: NREL-5MW low $I_{H,\infty}$.

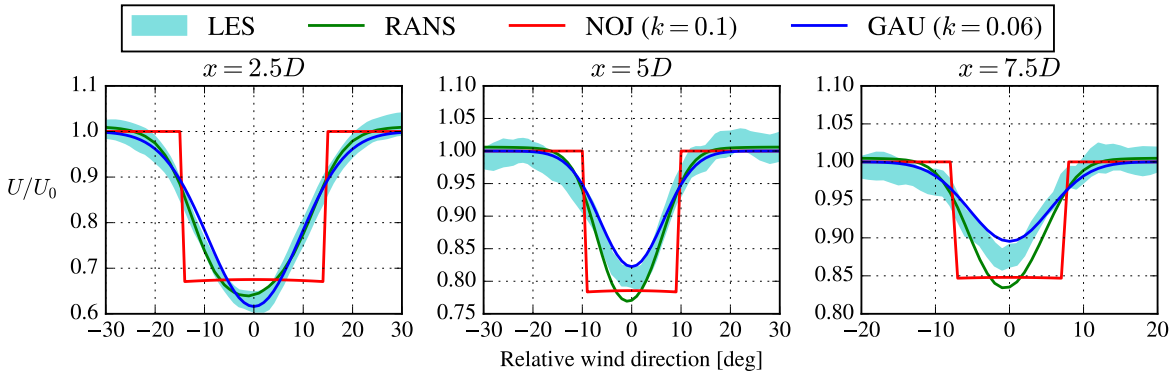

Figure 6: Case 6: NREL-5MW high $I_{H,\infty}$.

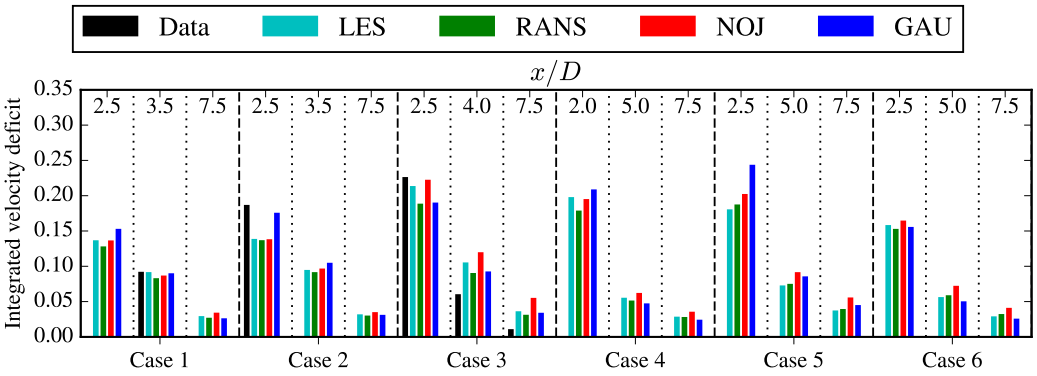

Figure 7: Integrated velocity deficit ($1/\int dy \int [1-U/U_0]dy$) of single wake cases (Cases 1-6).

3.1.2 Wind farm cases

The models results in the wind farm cases are post processed by a Gaussian filter, which represents the uncertainty of measured reference wind direction, as discussed by Gaumond et al. (2014). The chosen standard deviation for each case is based on van der Laan et al. (2015a), where the standard deviation in the Horns Rev I wind farm is a linearly increasing with the distance to the location of the measured reference wind direction. The Gaussian averaged (GA) post processed results are shown by dashed lines in Figures 8-18.

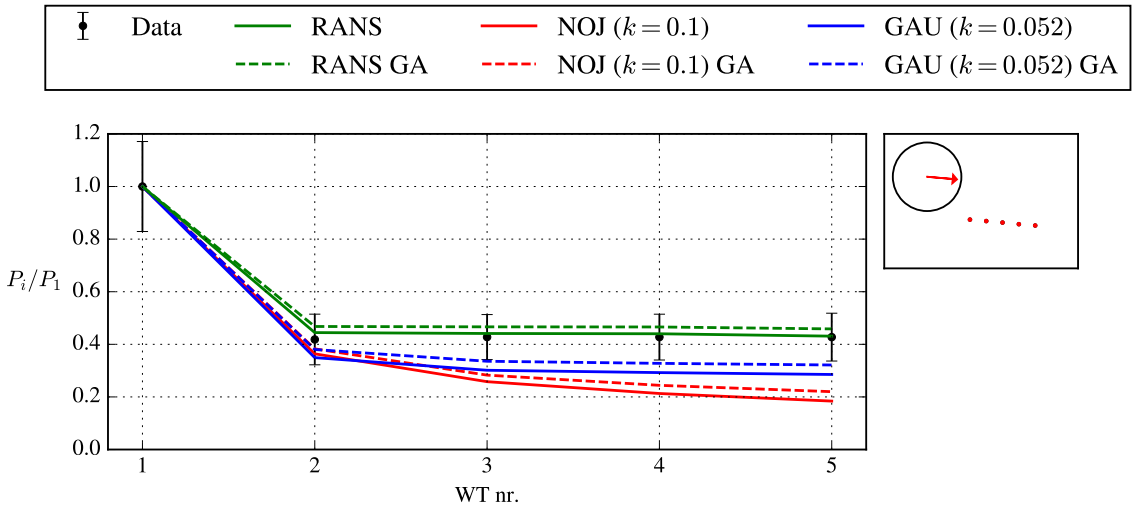

Figure 8: Case 7: Wieringmeer row.

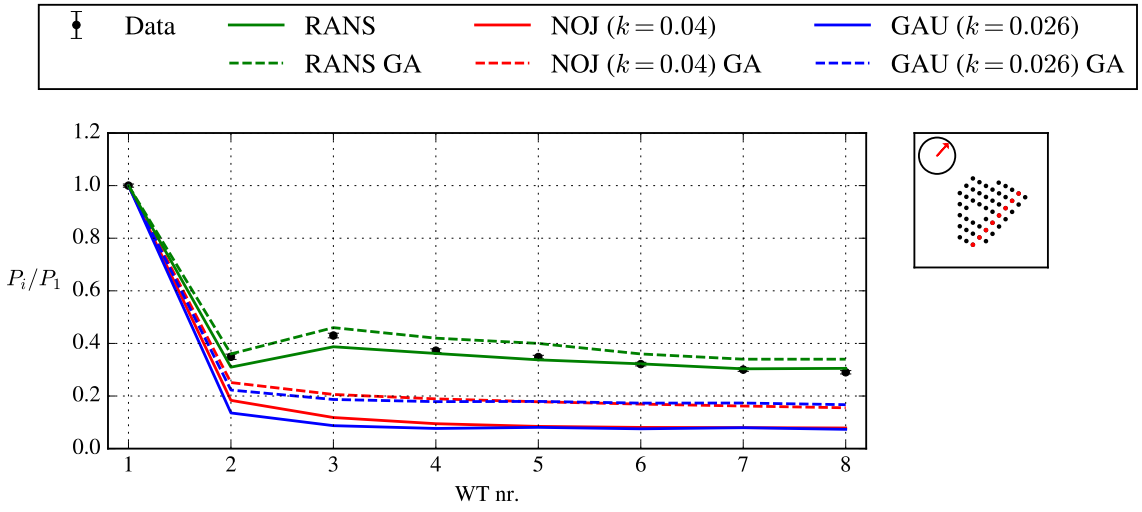

Figure 9: Case 8: Lillgrund Row B, for a wind direction of $222 \pm 2.5°$.

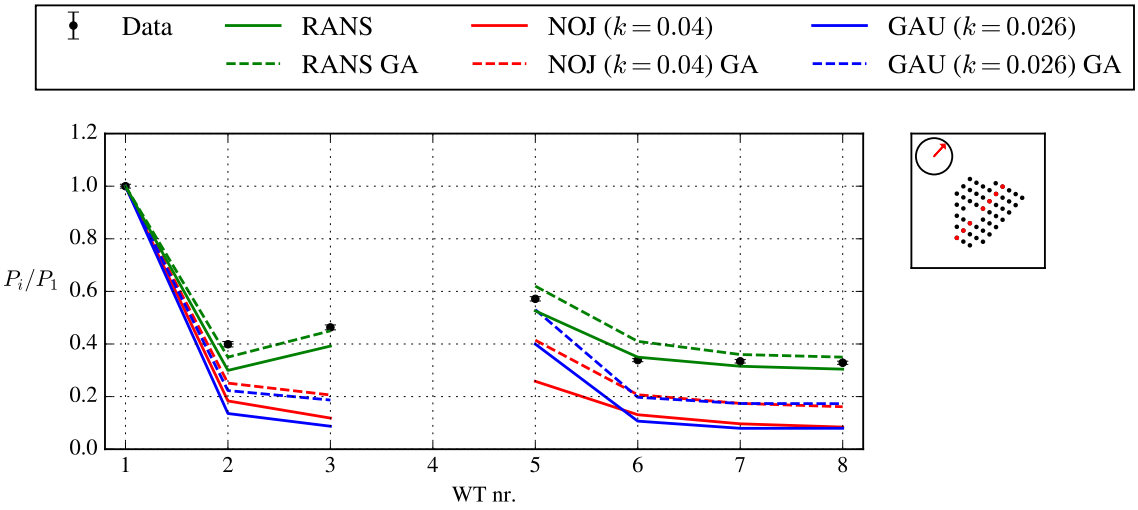

Figure 10: Case 8: Lillgrund Row D, for a wind direction of $222 \pm 2.5°$.

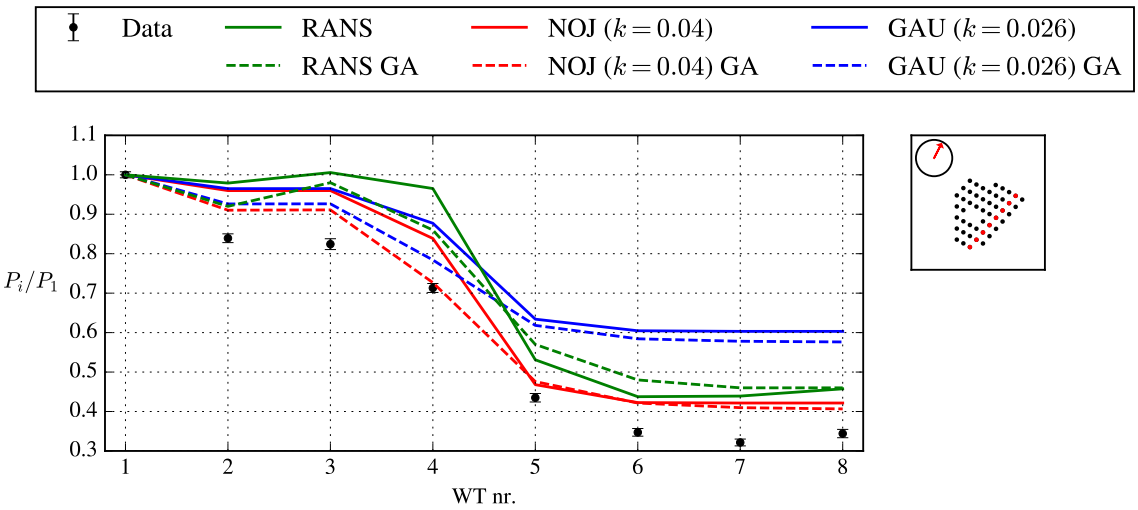

Figure 11: Case 9: Lillgrund Row B, for a wind direction of $207 \pm 2.5°$.

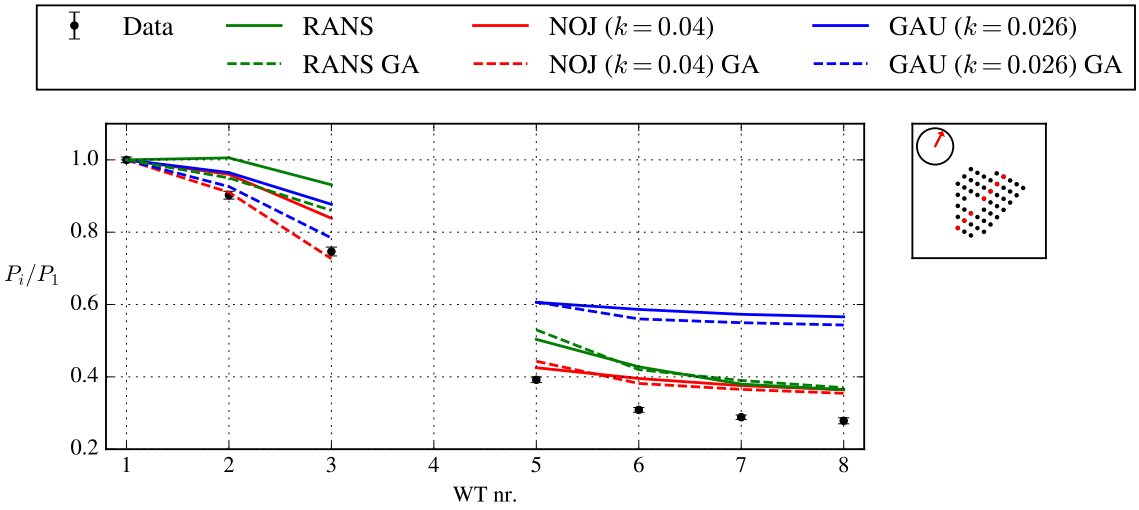

Figure 12: Case 9 Lillgrund Row D, for a wind direction of $207 \pm 2.5°$.

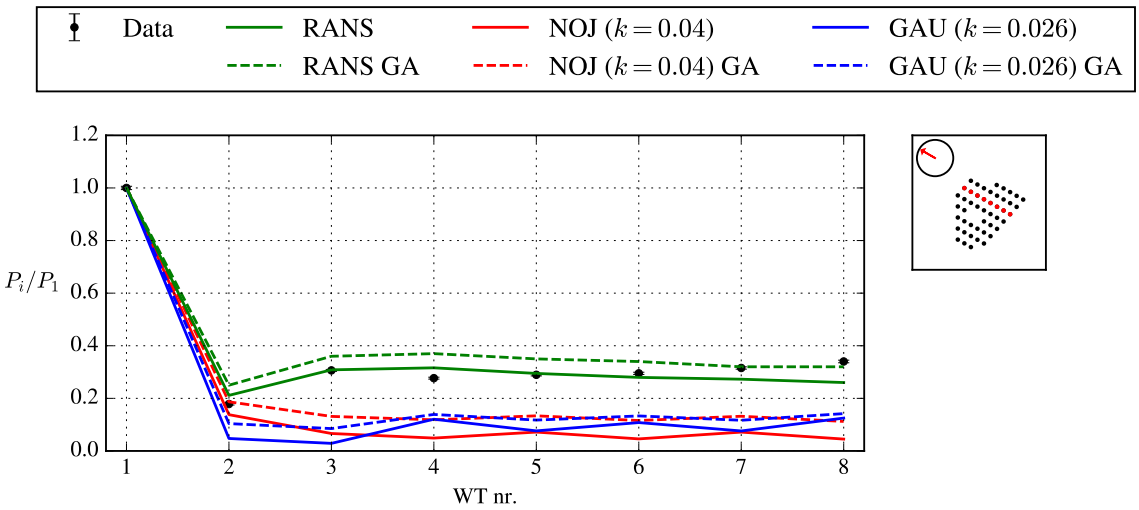

Figure 13: Case 10: Lillgrund Row 6, for a wind direction of $120 \pm 2.5°$.

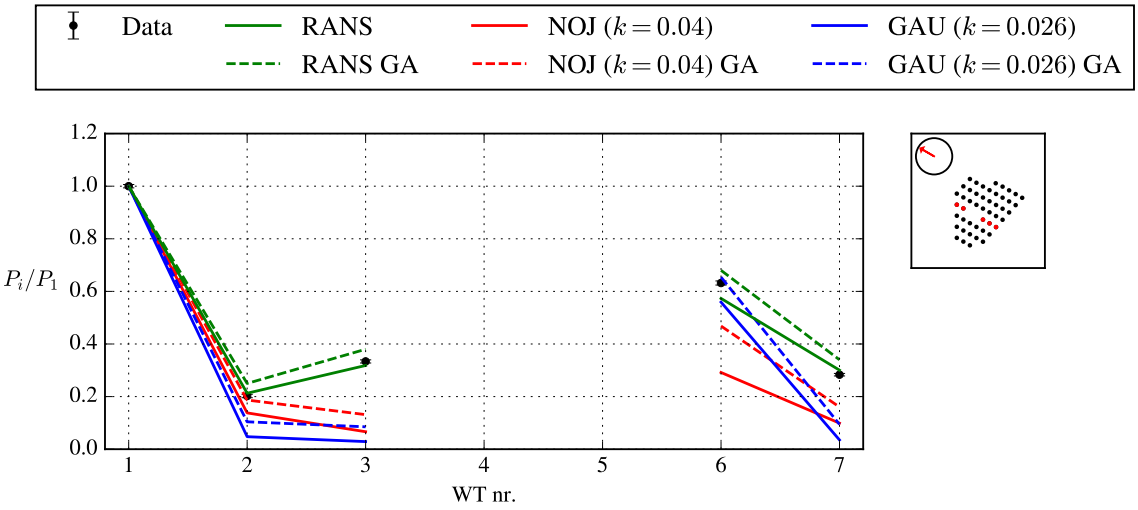

Figure 14: Case 10: Lillgrund Row 4, for a wind direction of $120 \pm 2.5°$.

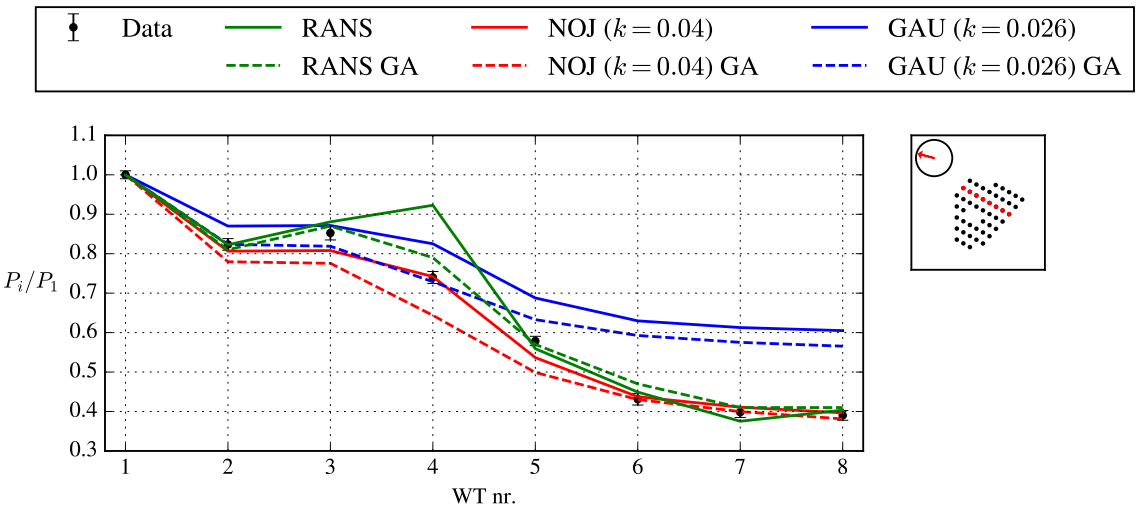

Figure 15: Case 11: Lillgrund Row 6, for a wind direction of $105 \pm 2.5°$.

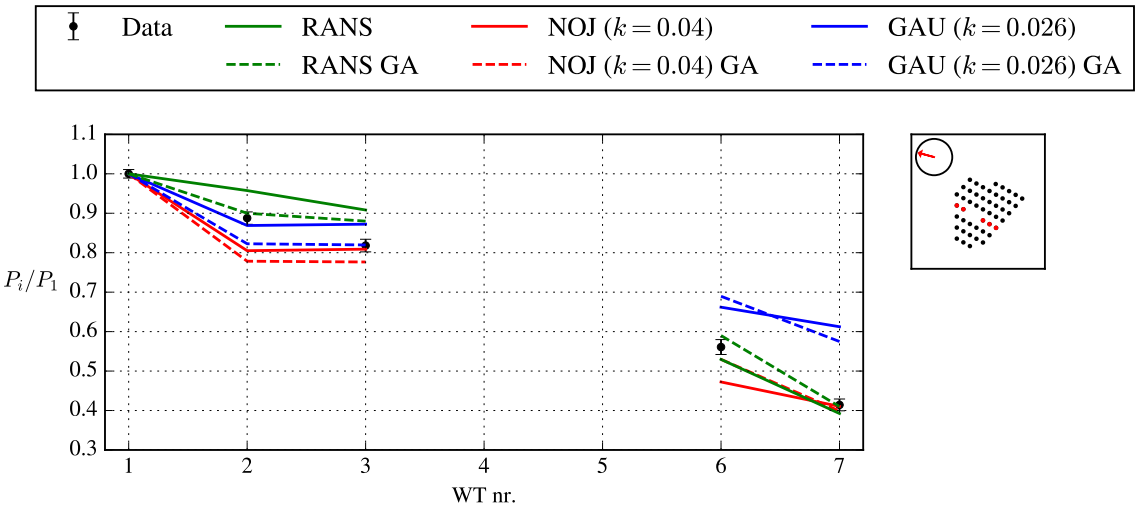

Figure 16: Case 11: Lillgrund Row 4, for a wind direction of $105 \pm 2.5°$.

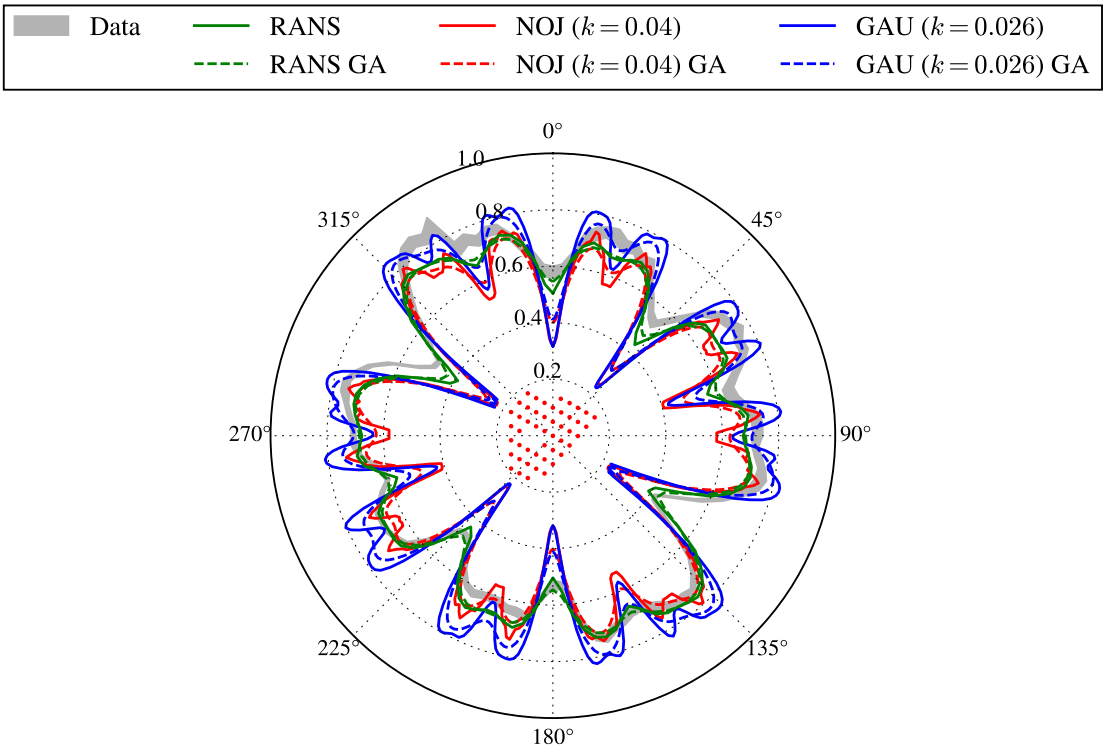

Figure 17: Case 12: Lillgrund wind farm efficiency.

	Measurement data	RANS	NOJ	GAU
Wind farm efficiency	0.66 ± 0.016	0.64	0.59	0.64
Relative error [%]	-	-3	-11	-2

Table 2: Case 12: Wind farm efficiency of the Lillgrund wind farm for uniformly distributed wind direction.

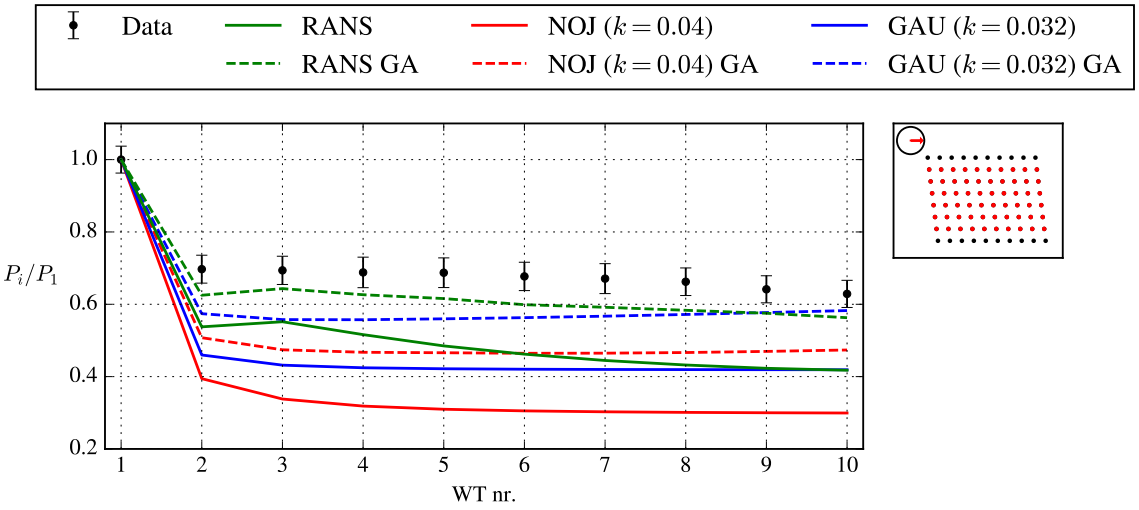

Figure 18: Case 13: Horns Rev I, average of inner rows, for a wind direction of $270 \pm 2.5°$.

References

Majid Bastankhah and Fernando Porté-Agel. A new analytical model for wind-turbine wakes. Renewable Energy, 70:116–123, 2014. URL http://dx.doi.org/10.1016/j.renene.2014.01.002.

M. Gaumond, P.-E. Réthoré, S. Ott, A. Peña, A. Bechmann, and K. S. Hansen. Evaluation of the wind direction uncertainty and its impact on wake modeling at the Horns Rev offshore wind farm. Wind Energy, 17(8):1169–1178, 2014. URL https://onlinelibrary.wiley.com/doi/abs/10.1002/we.1625.

N. O. Jensen. A note on wind generator interaction. Technical Report Risø-M-2411, Risø National Laboratory, Roskilde, Denmark, 1983.

Amin Niayifar and Fernando Porté-Agel. A new analytical model for wind farm power prediction. In Journal of physics: conference series, volume 625, page 012039. IOP Publishing, 2015. URL https://doi.org/10.1088/1742-6596/625/1/012039.

M. P. van der Laan, N. N. Sørensen, P.-E. Réthoré, J. Mann, M. C. Kelly, N. Troldborg, K. S. Hansen, and J. P. Murcia. The k-ε-f_p model applied to wind farms. Wind Energy, 18(12):2065–2084, December 2015a. doi: 10.1002/we.1804. URL https://onlinelibrary.wiley.com/doi/abs/10.1002/we.1804.

M. P. van der Laan, N. N. Sørensen, P.-E. Réthoré, J. Mann, M. C. Kelly, N. Troldborg, J. G. Schepers, and E. Machefaux. An improved k-ε model applied to a wind turbine wake in atmospheric turbulence. Wind Energy, 18(5):889–907, May 2015b. doi: 10.1002/we.1736. URL https://onlinelibrary.wiley.com/doi/abs/10.1002/we.1736.

DTU Wind Energy
Department of Wind Energy
Technical University of Denmark

Risø Campus Building 118
Frederiksborgvej 399
DK-4000 Roskilde
www.vindenergi.dtu.dk

DTU Wind Energy E-XXXX
ISBN: XXXX